Cassini plasma spectrometer measurements of Jovian bow shock structure

Karoly Szego, David T. Young, Bruce Barraclough, Jean-Jacques Berthelier, Andrew J. Coates, David J. Mccomas, Frank J. Crary, Michele K. Dougherty, Geza Erdos, Donald A. Gurnett, et al.

Cassini plasma spectrometer measurements of Jovian bow shock structure

Karoly Szego,[1] David T. Young,[2] Bruce Barraclough,[3] Jean-Jacques Berthelier,[4] Andrew J. Coates,[5] David J. McComas,[2] Frank J. Crary,[2] Michele K. Dougherty,[6] Geza Erdos,[1] Donald A. Gurnett,[7] William S. Kurth,[7] and Michelle F. Thomsen[3]

Received 3 June 2002; revised 18 March 2003; accepted 22 April 2003; published 18 July 2003.

[1] The Cassini spacecraft on its way to Saturn flew by Jupiter and crossed its bow shock more than forty times on the dusk-side of the planet, whereas the early missions targeting Jupiter explored the dawnside. Here we report the first results concerning these bow shock crossings, based on the measurements of the Cassini Plasma Spectrometer (CAPS), the magnetometer, and the radio and plasma wave science (RPWS) instrument. We present data for five bow shock crossings, one at about 1920 local time (LT), the other four between 2100 and 2130 LT, 47.5°–50° beyond terminator. During the flyby the solar activity was high and variable. The measurements confirm that the Jovian bow shock is huge, extending over 700 R_J down the flank; Cassini was the first to observe such distant shock features. The bow shock was turbulent and very dynamic and magnetic fluctuations were superimposed on the shock; the downstream ion distributions exhibited bimodal structure time to time. For all bow shock crossings the onset of ion thermalization was a clear shock signature supported by an electrostatic wave signal; thermalization can be used as a signature of the shock location even in those cases when the field data are rather smeared. The strength of the shock potential weakened toward more distant regions even if the local Mach number did not decrease. Reflected protons were not detected upstream above our current sensitivity limit, but the incoming solar wind fluctuated in the foot region. We argue that the Jovian bow shock is not always in a steady state, and some of the observations might be connected with this fact. *INDEX TERMS:* 2784 Magnetospheric Physics: Solar wind/magnetosphere interactions; 2154 Interplanetary Physics: Planetary bow shocks; 2164 Interplanetary Physics: Solar wind plasma; 2109 Interplanetary Physics: Discontinuities; *KEYWORDS:* Cassini, fields and particles, Jupiter, bow shock, solar wind parameters

Citation: Szego, K., et al., Cassini plasma spectrometer measurements of Jovian bow shock structure, *J. Geophys. Res.*, *108*(A7), 1287, doi:10.1029/2002JA009517, 2003.

1. Introduction

[2] The objective of this paper is to report the first results on the properties of the Jovian bow shock as observed during the flyby of the Cassini spacecraft. The results presented here are based on the data collected by the magnetometer, radio and plasma wave science instrument (RPWS), and the Cassini plasma spectrometer (CAPS) carried on board Cassini. The uniqueness of this data set is due to the favorable spacecraft orbit near Jupiter: in contrast to previous missions it skimmed the bow shock rather than crossing it quickly, and the craft spent a relatively long time in the different plasma regions close to it. More than forty bow shock crossings were recorded along the spacecraft orbit starting from the dayside and extending to the distant flank over more than three months. This allows the study of the giant Jovian bow shock under very special conditions, during high solar activity, not attained by other missions.

[3] Six spacecraft visited Jupiter before Cassini: Pioneer 10 and 11, Voyager 1 and 2, Ulysses, and Galileo. With the exception of Galileo, these spacecraft arrived at the planet between 1000 and 1100 local time (LT), the first four left it between 0200 and 1200 LT and explored the dawnside of the Jovian bow shock (that is, the other side than Cassini). Owing to the strong corotation of the Jovian magnetosphere, symmetry between the dusk/dawn sides cannot be taken for granted; therefore the Cassini data provide new information on the Jovian bow shock.

[4] Both Voyagers observed multiple inbound (between ~100 ~60 R_J around 1100 LT) and outbound bow shock

[1]KFKI Research Institute for Particle and Nuclear Physics, Budapest, Hungary.
[2]Southwest Research Institute, San Antonio, Texas, USA.
[3]Los Alamos National Laboratory, Space and Atmospheric Science Group, Los Alamos, New Mexico, USA.
[4]Centre d'Étude des Environnements Terrestre et Planetaires, IPSL, France.
[5]Mullard Space Science Laboratory, University College London, London, UK.
[6]Imperial College, London, UK.
[7]Department of Physics and Astronomy, The University of Iowa, Iowa City, Iowa, USA.

0148-0227/03/2002JA009517

crossings (between ~220 ~280 R_J along the flank). Comparing these locations with the position of magnetopause crossings, *Scarf et al.* [1981] noted that the location of the boundaries vary widely in response to the presumed changes in the solar wind pressure and suspected that other causes may also play a role (such as interplanetary events). *Scudder et al.* [1981] reported a nearly perpendicular inbound shock for Voyager 1 with abrupt, near maximal (~4) density jumps, and a ~10 electron temperature jump. (During that particular crossing the SW bulk velocity was ~400 km/s, electron density ~0.5 electron cm^{-3}, $T_e/T_p = 2.5$, and $\beta \sim 2$. The core SW electron temperature was ~3 eV, with a suprathermal component $T_e \sim 43$ eV and 4% of core density). The plasma wave measurements [*Scarf et al.*, 1981] found intense broadband turbulences in a thin layer of the shock, preceded by intense bursts of electron plasma oscillations upstream. The outbound bow shock crossings were frequently weak and diffuse in the wave data, though still clearly identifiable. The Voyager observations confirmed that the Jovian magnetosphere is easily compressible.

[5] The Ulysses inbound shock was quasi-parallel (36°) at 113 R_J, and three quasi-perpendicular crossings were detected outbound between 109 and 149 R_J [*Balogh et al.*, 1992]. The Ulysses Radio and Plasma Wave experiment [*Stone et al.*, 1992] confirmed the presence of electrostatic bursts in the frequency range between 10 Hz and 10 kHz with the largest amplitude near the ramp. The solar wind plasma experiment [*Bame et al.*, 1992] detected at the inbound shock crossing a jump in electron density from 0.06 to ~0.15 cm^{-3} and a temperature jump from ~0.2 eV to ~1.5 eV.

[6] *Kivelson et al.* [1997] compared the Galileo crossings with the results of the other missions. They concluded that the Jovian magnetosphere can experience large changes in its magnetic configuration and attributed it to the changes of the solar wind dynamic pressure.

[7] On the basis of the bow shock crossing locations of these missions, *Huddlestone et al.* [1998] were the first who attempted to find an average shape of the Jovian bow shock. They have also pointed out the variability of the shock front due to the rapidly changing magnetodisk of Jupiter. None of the published papers discussed the details of the shock structure.

[8] Hybrid simulations of high Mach number bow shocks [*Leroy et al.*, 1982; *Quest*, 1985] indicated that shocks above a (second) critical Mach number (>13) cannot be stationary; neither conventional energy dissipation mechanisms nor additional dissipation due to the reflected ions provide adequate dissipation required for a steady state. This, for instance, may lead to a nonstationary situation and may cause fluctuations, e.g., in the reflected particle distributions. In these papers it was also suggested that observations at Jupiter might help to resolve this issue.

[9] Several papers were published to describe the physics of the foot region of the shock [see, e.g., *Moses et al.*, 1985, and references therein], but as we shall discuss the CAPS foot observations in a separate paper, we do not go into details here.

[10] The goals of this paper are threefold: (1) to provide a phenomenological description of the Jovian bow shock in a region that has not been investigated previously, (2) to contribute to the analysis of the variability of the Jovian bow shock, and (3) to discuss a few particular questions specified later. Most of the bow shock crossings we observed do not follow simple patterns, and at this point it is beyond our understanding to explain all the details of the plasma structures detected. In this paper only a part of the observations presented are interpreted. However, by selecting a few representative examples we would like to provide material for further studies by other teams as well.

[11] In the next section we describe the instrumentation used for data acquisition, Section 3 summarizes the solar wind conditions during the flyby; the two subsequent sections are devoted to describe bow shock properties, and we present our summary and conclusions in the last section.

2. Instrumentation

[12] The Cassini spacecraft, launched to study the environment of Saturn, flew by Jupiter on its way to tap the planet's gravity field. The closest approach took place on 30 December 2000. The CAPS instrument has three independently operated sensors: the ion mass spectrometer (IMS) designed to analyse ion composition and plasma dynamics, the electron spectrometer (ELS), and the ion beam spectrometer (IBS) to measure narrow, beam-like distributions without mass separation. CAPS is described in detail by *Young et al.* [1998, 2002]. The magnetometer (MAG) has several modes of operation; we use here 1-s or 4-s resolution data, depending on telemetry rate [see *Dougherty et al.*, 2002]. The radio and plasma wave science instrument (RPWS) [*Gurnett et al.*, 2002a, 2002b] acquires amplitudes of wave electric fields from approximately 1 Hz to 16 MHz and wave magnetic fields from approximately 1 Hz to 12 kHz providing a spectrum once per 32 to 64 seconds, depending on the instrument mode. The RPWS uses three monopole electric antennas and a set of triaxial search coils for sensors. For selected intervals, higher resolution observations are made with wideband and waveform receivers; however, such measurements are not included in this paper.

[13] During its flyby at Jupiter, Cassini performed complex scientific observations which required frequent changes in the spacecraft orientation; therefore the solar wind was not always in the field of view of CAPS (ELS sees the solar wind as the thermal velocity is higher for electrons), and instrument telemetry modes also varied. In this paper we report results from periods when the plasma flow was in the field of view of CAPS both before and after the bow shock crossings, and the telemetry rate for CAPS was 2 kbps. In this telemetry mode CAPS-IMS resolves energy in 64 logarithmic steps between 1 eV and 50 keV and elevation in four equal, 40° wide angular channels; one such spectrum was collected in 16 s. For CAPS-ELS [*Linder et al.*, 1998] the 64 logarithmic energy steps are between 1 eV and 30 keV, the 160° elevation field of view is split into 20° wide angular channels, and one such spectrum was collected in every 32 s (it is the modes used for many of the crossings which degrades the time resolution from the basic 2 s for an ELS sweep). The ion beam spectrometer, CAPS-IBS, has three entrance apertures offset by 30°, and each field of view is 1.5° × 150°. CAPS-IBS collected all ions in 256 specially selected narrow energy steps between ~200 eV and ~9.5 keV with energy resolution $\Delta E/E = 0.015$; one

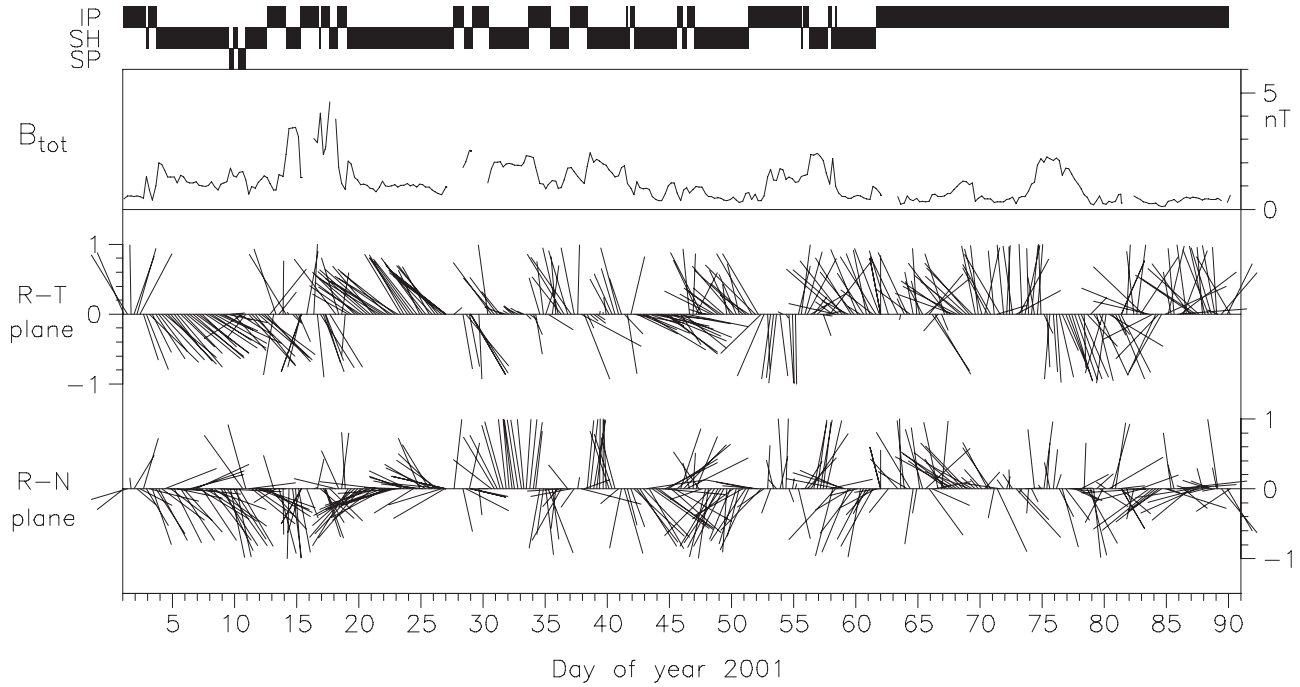

Figure 1. Six-hours averaged magnetic field vector directions are shown in the RTN frame of reference, as measured by the magnetometer onboard Cassini in 2001, between DOY 001 and 090. The approximate time of the bow shock crossings are shown in the upper plot (W. S. Kurth et al., private communication, 2002), the abbreviations denote the different plasma regions: IP = interplanetary (upstream), SH = magnetosheath, SP = magnetosphere. Below the magnitude of the magnetic field is displayed; then the field vector directions in the R-T (∼close to the Solar ecliptic plane) and R-N planes are shown.

full spectrum was taken in 0.5 s. In the 2 kbps telemetry mode, 16 sweeps were added during a 32-s long time interval. The field of view in the azimuth direction was 11° for IMS, 5° for ELS, and 1.5° for IBS. The whole CAPS package can be actuated around a rotation axis parallel to the symmetry planes of the IMS and ELS field of views and oriented perpendicular to the symmetry axes of these instruments FOV.

[14] The actuator performed windshield-wiper-like motion in a variable-length interval, the highest angular velocity being about 1° s^{-1}; the actuator-plane position defines the azimuth plane of the look direction (the actuation is in X-Y plane in the spacecraft coordinate system; 0° azimuth corresponds to viewing out along the Y axis of the spacecraft coordinate system). In the 2 kbps telemetry mode, azimuth values were summed for IMS during a 16-s long time interval, for ELS and IBS in a 32-s long interval; this is the best time/space resolution in this mode of operation. In the solar wind (SW), however, if the plasma flow was stable for a longer period of time, even a few-degree azimuth resolution could be achieved during multiple scans exploiting the fact that the actuator motion is not in phase with the data acquisition time-interval. A detailed description of IBS operation was published by *Vilppola et al.* [2001].

3. Solar Wind at Jupiter, Global Features

[15] Cassini encountered Jupiter during a period of high solar activity, and according to the investigators of the magnetometer onboard Ulysses, two magnetic sectors were present on the Sun up to high latitudes in the year 2000 and at the beginning of 2001 [*Smith et al.*, 2001]. The picture emerging from this appears to be consistent with a single warped current sheet tilted slightly to the rotation axis of the Sun. The 6-hour averaged magnetic field vectors in the RTN coordinate system for the first 90 days of 2001, shown in Figure 1, indicate very dynamic magnetic field variations, and the out-of-ecliptic field components (N-direction) were frequently high. (The RTN coordinate system is defined as follows: the R unit vector points from the Sun to the spacecraft direction, the T unit vector points to the $\mathbf{\Omega} \times \mathbf{R}$ direction where $\mathbf{\Omega}$ is the Sun spin axis, and the N unit vector completes the right-hand system. When R is in the ecliptic plane, N is almost parallel to the ecliptic north, the difference being less than 8°. On DOY 055 and DOY 075 a sector boundary crossing is evident from the sudden change of the field components in the ecliptic plane, and the relative stability of its direction between these dates. Large-scale structures with a relative stability of the direction of the IMF in the ecliptic plane can also be found between days 3 and 13, 17 and 27.

[16] The "nominal" solar wind parameters at Jupiter are $B \sim 1.2$ nT, $n \sim 0.3–0.4$ particle cm^{-3}, $v \sim 400$ km/s, the Parker spiral angle between the SW velocity and the magnetic field vector being ∼79° (see, e.g., chapter 6.4.2 of *Cravens* [1997]). We derived the 1-hour averaged solar wind velocity vectors by fitting a Maxwellian distribution to all IMS data points. Because the actuator did not move in

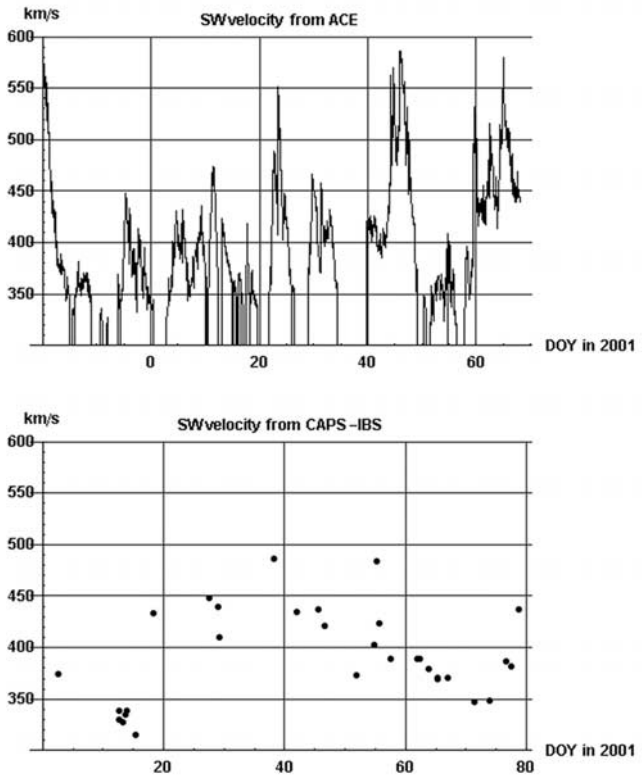

Figure 2. The variation of the 1-hour averaged SW velocity at Jupiter during the first 80 days of 2001 based on 2 kbps IBS data (lower panel) and at Earth starting 20 days earlier using the SWEPAM instrument data onboard ACE (upper panel).

phase with the data collection time interval, this allows a relatively accurate determination of the x and y components of the SW velocity in the spacecraft frame of reference if the SW is stable. As we have mentioned, the resolution along the spacecraft z-direction was coarse (40°); therefore the z-component of the velocity vector in the spacecraft coordinate system has much higher error than the two other components. The 1-hour averaged total velocity of the SW was also derived from the IBS data. These values are plotted in Figure 2. In the same figure we have also exhibited the SW velocities at Earth, as obtained by the SWEPAM instrument onboard ACE, publicly available from www.srl.caltech.edu/ACE/. This supports earlier recommendations [*Huddlestone et al.*, 1998] that with appropriate time shift the SW parameters measured at the Earth can be used as proxy if needed because the Earth and Jupiter were almost aligned during this period.

[17] We have two methods to obtain the SW temperature. One is to fit Maxwellians to the IBS energy distribution. The second is to exploit the azimuth extent of the plasma distributions. Assume that the SW distribution can be described by a Maxwellian centered on the bulk velocity vector $\{v_x, v_y, v_z\}$ with v_T as half-width, where v_T is the SW thermal velocity. To take into account the smearing effect of the 11°-wide field of view of the IMS sensor in azimuth, we convolute the instrument response function with the SW distribution in the azimuth direction (but not in elevation direction because the FOV resolution in elevation is wider than the angular distribution of the solar wind ions). With good enough accuracy, the azimuth response function can be approximated by a Maxwellian centered on the actual view direction, with half width $|v_{bulk}|\ \tan(3°)$. The convolution of two Maxwellian is again a Maxwellian with a modified thermal velocity $v_{T,mod} = (v_T^2 + v_{bulk}^2 \tan^2(3°))^{1/2}$. Therefore the SW temperature was obtained by integrating the counts over v_z and $(v_x^2 + v_y^2)^{1/2}$, assuming a Maxwellian distribution function with $v_{T,mod}$ in the x-y directions.

$$\int v\,dv \int dv_z \frac{1}{\pi^{3/2} v_{T,mod}^2 v_T} exp\left[-\frac{(v_z - v)^2}{v_T}\right.$$

$$\left. \cdot\ exp\left[-\frac{\left((v\cos\varphi - v_{x0})^2 + \left(v\sin\varphi - v_{y0}\right)^2\right.}{v_{T,mod}^2}\right]\right.$$

$$= \frac{1}{2\pi}\left[exp\left(-\alpha^2\right) + exp\left(-\alpha^2 sin^2(\varphi_{max} - \varphi)\right)\right.$$

$$\left. \cdot\sqrt{\pi}\alpha\, cos(\varphi_{max} - \varphi)[1 + erf(\alpha\, cos(\varphi_{max} - \varphi))]\right.$$

where $\alpha = \frac{\sqrt{v_{x0}^2 + v_{y0}^2}}{v_{T,mod}^2}$, and $\varphi_{max} = arc\,cos\left(\frac{v_{y0}}{\sqrt{v_{x0}^2 + v_{y0}^2}}\right)$.

[18] Then using the calculated v_{x0} and v_{y0} velocity components, we fitted an overall scale factor and v_T to the integrated counts. An illustration of the SW temperature fit is shown in Figure 3. The temperature obtained this way is somewhat higher than the temperature obtained by fitting Maxwellian directly to the IBS data. Despite this small discrepancy (to be clarified in the future) we shall use both methods because it does not affect the observations presented in this paper.

[19] During the 3 month long interval shown in Figure 1 the solar wind exhibited high variability; the presence of

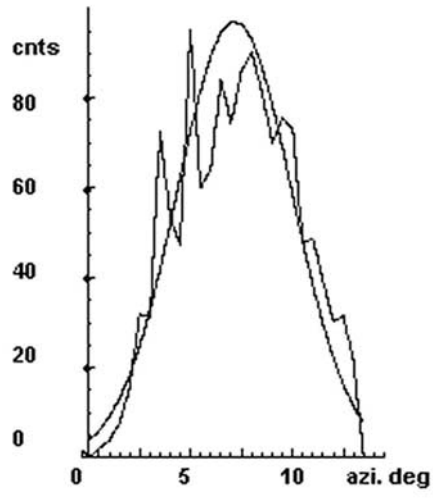

Figure 3. The count-azimuth distribution of the SW on DOY 012 between 1500 and 1600 UT. The horizontal axis is azimuth in degrees; the vertical axis displays counts. The fit corresponds to v_x = 257 km/s, v_y = 127 km/s, and v_{bulk} = 298 km/s in the spacecraft frame of reference, and $v_T \sim$ 12 km/s.

small and mesoscale structures was evident in the flow, including interplanetary shocks. We illustrate these by some characteristic events. On DOY 002 and 003, before Cassini crossed the bow shock, the magnitude of the SW velocity was about 320–330 km/s, and the SW was cold, with $v_T \sim 10 \div 12$ km/s. The structure of the shocked solar wind between DOY 003 and 012 and the differences of the boundary positions as measured by Galileo and Cassini were interpreted by *Hill* [2002] as the effect of an interplanetary shock that passed Jupiter. At the end of the DOY 012, at about 2200 UT, the T and N components of the magnetic field vector changed sign, and a hot SW stream crossed the spacecraft, and v_T jumped to $25 \div 30$ km/s without any significant change in the magnitude of the velocity. Cassini probably crossed another interplanetary shock on DOY 015 $\sim$ 1140 UT, shown in Figure 4, the SW energy and temperature jumped up together, with a significant change in the magnetic field data. In the RPWS data the IP shock is seen in the lower frequency range. Several other IP shocks were seen during this 90 day long period of time as well.

[20] The increase in SW velocity and temperature around DOY 018 (cf., Figure 2) is probably the signature of a sector boundary crossing. Between DOYs 040 and 060 the magnetic field was fluctuating even in a 1-hour long scale, and a sector boundary crossing is likely on DOY 055 (see Figure 1). It seems likely that between DOYs 052 and 055, Cassini was in the midst of hot SW. The SW became slower and colder around DOYs 060 and became faster and hotter close to the sector boundary crossing around DOY 075.

4. Bow Shock on DOY 012

[21] Cassini encountered the Jovian bow shock first time on 28 December 2000, ~0419 UT, but the first bow shock crossing with full CAPS coverage took place on 12 January 2001, ~1420 UT, at a distance of about 224 R_J (1 R_J = 71,492 km) from the planet, ~24° behind the terminator line in the orbit plane, and the spacecraft was ~0.7° below the solar equatorial plane. During the time interval discussed here the CAPS instrument was actuated around an axis perpendicular to the ecliptic plane, from −79° to 102° in azimuth, the solar wind arrived from the 56°–70° azimuth interval in the spacecraft coordinate system. In the RTN frame of reference the unperturbed SW velocity was about $\mathbf{v}_{SW}$ = {315, 14, 82} km/s as derived from the CAPS-IMS SW spectra measured between 1500 and 1600 UT when the wave activity was quiet. The variation of the magnetic field vectors in RTN and the bulk plasma velocities as derived from IBS are shown in Figure 5.

[22] The shock crossing is evident from the steep jump of the magnetic field at 1420 UT. In general the magnetic field near the bow shock is seldom stable; therefore we describe how we obtained the shock normal. Two methods were used to determine the shock normal from the measured magnetic field data. One is based on the coplanarity theorem, by taking the upstream and downstream averages of the magnetic field vectors, $\mathbf{B}_u$ and $\mathbf{B}_d$ and calculating the shock normal $\mathbf{n}$ as the unit vector parallel to $(\mathbf{B}_u - \mathbf{B}_d) \times (\mathbf{B}_u \times \mathbf{B}_d)$ or else $\mathbf{n}.(\mathbf{B}_u \times \mathbf{B}_d) = 0$. The other method used the minimum variance technique. The normal is expected in the plane perpendicular to the maximum variance direction.

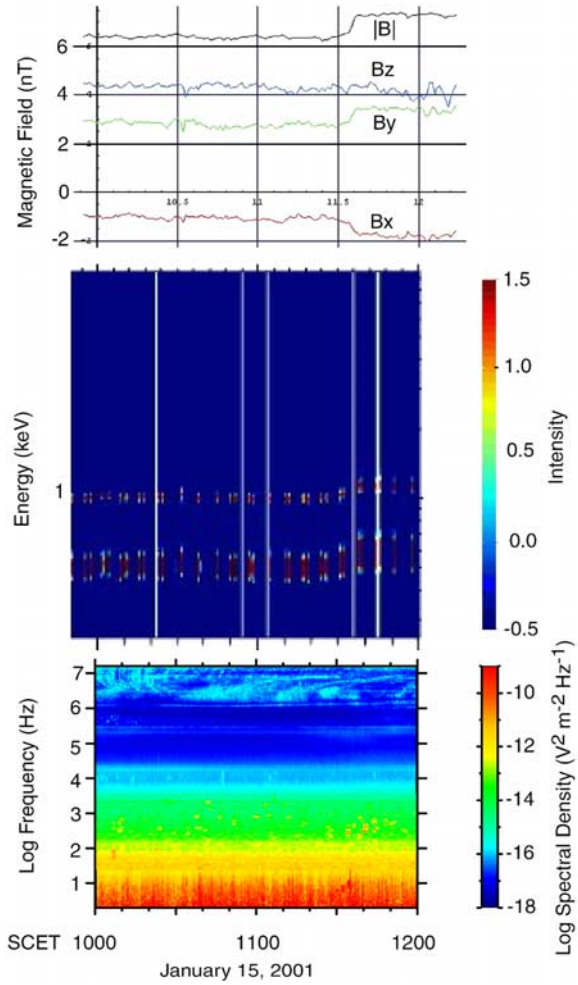

Figure 4. An interplanetary (IP) shock on DOY 015 between 1000 and 1200 UT. The upper plot shows the magnetic field components in the spacecraft frame of reference (B_x is red; B_y is green, shifted up by 2 nT; B_z is blue, shifted up by 4 nT) and the total field (black) shifted up by 5 nT. The middle plot shows the IBS energy spectra, whereas the lower plot exhibits the RPWS data for the same time interval.

The measured field vectors were projected to the plane, and the normal was selected by taking the direction parallel to the average of those vectors. In both methods the time interval of the shock transition was discarded.

[23] Both methods give uncertain results close to either quasi-parallel or to quasi-perpendicular shocks. Further, there is a danger, especially with the variance technique, that the calculation of normal can be misled by large amplitude waves not associated with the shock transition. We have checked the consistency of the calculation by selecting various time intervals for the upstream, downstream, and shock transition regions. The normal is acceptable if the two methods give similar results and which are relatively insensitive for the selected time intervals.

[24] On DOY 012 the shock was quasi-perpendicular, $\theta_{Bn} > 80°$, the shock normal in RTN pointed to {−0.62, −0.76, 0.18}, so the spacecraft velocity was almost perpendicular to the shock normal, indicating that the space-

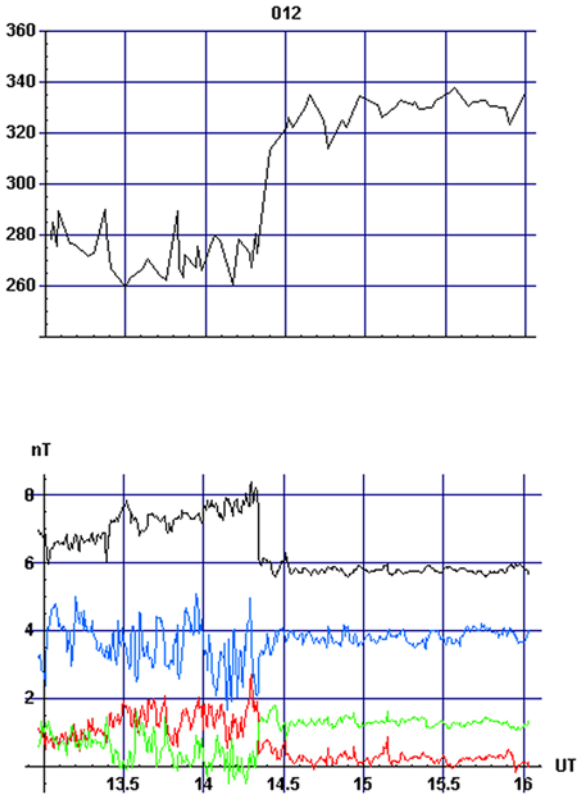

Figure 5. The upper plot shows the bulk plasma velocity on DOY 012 between 1300 and1600 UT; the lower plot exhibits the magnetic field components in RTN for the same time period. The plot label of Figure 4 contains the explanation of color coding and level shifts for the magnetic field components.

craft was really "skimming" the shock. Despite that, the crossing was very fast; according to the hi-res magnetic data, the spacecraft crossed the shock ramp in 8 s. The shock normal direction for this crossing agrees reasonably well with the shape model of *Huddlestone et al.* [1998].

[25] In the wave data the signature of this bow shock crossings is very clear: it is a sharp signal outstanding in the proton plasma frequency region ($f_p = 210\, n^{1/2}$ Hz), extending up to 1000 Hz. Similar wave signature in the ramp was observed during the Voyager mission as well [*Moses et al.*, 1985; *Scarf et al.*, 1987]; it is believed that this is due to electrostatic ion waves [*Wu et al.*, 1984]. The characteristics of this signal are not different from the one observed at Earth by RPWS on Cassini [*Moses et al.*, 1990; *Kurth et al.*, 2001]. This is a good example that certain shock features are independent of the obstacle. The shock is also clearly seen in the CAPS-IBS data: the ion thermalization downstream is an excellent signature of bow shock crossings. These are illustrated in Figure 6, showing the IBS energy spectra together with the wave data measured in the same time interval.

[26] The wave spectra seen in Figure 6 show intense peaks upstream around 10 kHz; we identify those with Langmuir waves. From these and also from the IBS spectra an approximate upstream density of about 0.5–1 cm^{-3} is obtained. The upstream electron temperature, as derived from the SW electron spectra, was about 2.6 eV. Using the measured $B_{tot} \sim 0.8$ nT shown in Figure 5, we get $v_A \sim 32$ km/s; hence the SW Mach number was $M_A \sim 10$ (for the velocity component perpendicular to the bow shock $M_A \sim 7$). The spacecraft velocity was {9.3, −5.1, 0.6} km/s in RTN. According to hybrid simulations [*Leroy et al.*, 1982], the width of the foot of quasi-perpendicular shocks is about the proton gyroradius, ~1500 km for the nominal SW parameters, and the shock width is about the proton's inertial length, ~300 km. We conjecture from this sharp transition that in this period the shock ramp passed over the spacecraft with a ~30 km/s velocity.

[27] Four downstream ion distributions are shown in Figure 7 as a function of velocity. Thermalization increases farther from the shock front (the distribution "1" is the farthest); the change in the peak velocity is significant but does not show a clear trend. The presence of a non-Maxwellian tail is evident even from visual inspection of the data. Note the absence of a downstream shoulder, typically seen in Earth's magnetosheath, due to reflected ions.

[28] We have solved the Rankine-Hugoniot relations for this transition (being aware that this is only an approximation for the plasma flow we investigate), using the measured upstream parameters and the measured downstream magnetic field values. This yields for the downstream plasma parameters $\rho_{down}/\rho_{up} \sim 2.74$, $v_{down} = \{233, -66, -96\}$ km/s equivalent to a downstream bulk energy ~360 eV, and a bulk velocity ~260 km/s, agreeing reasonably well with the data shown in Figure 7. For the total downstream plasma temperature the R-H conditions predict 44 eV. The downstream electron temperature from ELS data is about 11 eV, leaving ~33 eV for the downstream ion temperature. The proton temperature can be assessed also from the azimuth extent of the distribution, yielding ~24 eV, as can be seen

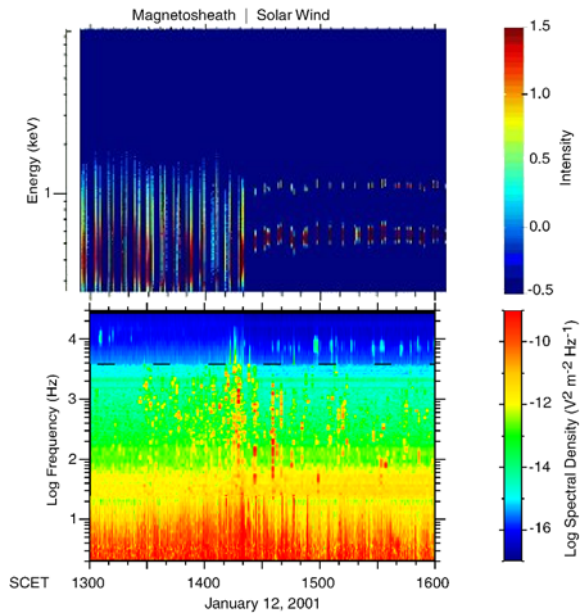

Figure 6. The upper plot displays the IBS counts on DOY 012 between 1300 and 1600 UT; time is shown on the horizontal axis. The vertical axis is energy in log eV; color represents log count number marked as "intensity." The lower plot is the wave spectrum for the same time interval, measured by RPWS. The vertical axis shows wave frequency; color is wave intensity.

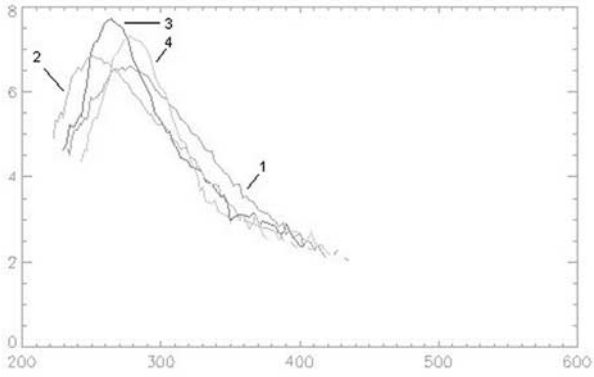

Figure 7. IBS ion log-distributions as a function of velocity measured downstream at 1403 UT (between actuator angles 31° and 64°) (1), 1410 UT (39°–71°) (2), 1417 UT (47°–79°) (3), and 1419 UT (50°–83°) (4). The horizontal axis displays velocity in km/s. The BS crossing took place at ~1420 UT.

also in Figure 7. The angle between the upstream and downstream velocities is about 18°; this agrees reasonably well with the 20° velocity deflection derived from actuator motion. The plasma motion obtained from the R-H relations reproduces quite well the observed bulk behavior downstream.

[29] It is more difficult to understand why we did not detect particles reflected back from the shock front. Both the flyby geometry and the FOV of the CAPS IMS and IBS sensors would have allowed to detect specularly reflected particles (in the vicinity of −30° actuator angle) or particles streaming along the upstream magnetic field (in the −30°–0° actuator range) but upstream no single count was detected outside the SW flow direction; also we do not see downstream shoulder. On the other hand, other evidences strongly suggest their existence:

[30] 1. The lower hybrid waves shown in Figure 6 in the foot region are very likely excited by reflected ions; especially intense waves are seen between 1430 and 1440 UT, 1500 and 1510 UT, and 1530 and 1540 UT.

[31] 2. The deceleration of the SW between the shock ramp and 1435 UT is very likely due to the increased ion population in the foot.

[32] One possible explanation, supported by test particle simulations, is that the reflected particles expand very quickly in phase space, both in the configuration and in the velocity space resulting in a flux below our sensitivity threshold. The intensive lower hybrid waves heat the incoming SW; such a heating is evident in Figure 6 around 1440 UT and 1540 UT as well. Even in these cases we did not see direct evidence of back-scattered particles.

[33] A related question is the observation of particles accelerated at the shock front. Shock acceleration processes, e.g., shock surfing, and shock drift acceleration were compared using a hybrid code for quasi-perpendicular shock by *Lever et al.* [2001]. Although in that study the incoming flow was a pickup ion shell, the conclusions are applicable to this case as well. An important conclusion was that the type of the acceleration mechanism for any given particle is defined by the kinetic parameter values valid at the first encounter of the given particle with the bow shock. Whereas accelerated and reflected particles were not seen upstream by CAPS, we believe that the high energy tail of the ion distributions downstream, shown in Figure 7, is due to ions accelerated at the shock front. These ions lose energy while crossing the shock ramp due to the anomalous resistivity resulting from wave-particle interaction [cf., *Leroy et al.*, 1982], but they reach the downstream region with energies still exceeding the upstream SW energy. Comparing to the velocity gains obtained by those simulations, the gains we detected are modest. Shock surfing leads to high velocities, and it is effective for narrow foot and low incoming velocity; therefore we conclude that shock surfing was not dominant at this crossing.

[34] Magnetic waves are seen superimposed on the shock. The wave structure is more clearly seen if we plot the endpoints of the magnetic field vectors in the system of reference where the shock transition is parallel to the x-axis. This is shown in Figure 8. The B_y–B_z hodogram indicates linear polarization in the downstream region.

5. Bow Shock on the Flanks

[35] In this section we discuss four other bow shock crossings, on DOY 042 between 0430 and 0500 UT inbound, on DOY 045 between 1400 and 1430 UT outbound, on DOY 055 between 1400 and 1430 UT inbound and ~1630 outbound, and on DOY 057 around 1430 UT; at a distance of 576, 618, 744, and 770 R_J, and at angles 47.5°, 48.3°, 49.8° and 50° behind terminator, respectively. For these bow shock crossings, the IBS energy-time spectra, the bulk plasma velocity, the magnetic field vectors, and the waves as measured by RPWS are shown in Figures 9–12, respectively.

[36] The shock crossings are evident by the onset of strong proton thermalization in the IBS energy-time spectra; in the RPWS this onset is always accompanied by a reasonably strong electrostatic signal, similar to the one shown in Figure 6. However, it would be very difficult to find the shock location only from the wave and magnetometer data. The variation of the bulk ion velocity shows a similar ''smeared'' picture; the quiet upstream and downstream regions are separated by hours.

[37] The solar wind velocities in RTN coordinates were (419, −88, −93), (407, −133, 16), and (404, −129, 6) km/s, respectively, for DOYs 042, 045, and 055; we could not derive the velocity vector for DOY 057 owing to the unfavorable spacecraft orientation. The Alfven velocity for these days was ~22 km/s, ~22 km/s, and ~50 km assuming 0.7 particle density per cc. (The density values were derived from the Langmuir waves; see section 4.) The large off-radial SW velocity components are to be noted; these are due to the relatively high z-component of the velocity in the spacecraft frame of reference. As the sampling in this direction (in the elevation direction) is coarse, these values might have been overestimated. The extent in azimuth of the upstream proton distributions were 18°, 18°, 17°, and 18°, respectively, leading to ~20 km/s (~4 eV) thermal proton velocities upstream. On these days the SW was not fully in the CAPS field of view; a small portion of it (maximum 5°) might have been missed at peak actuator angles. During the first three shock crossings the CAPS sensors were actuated

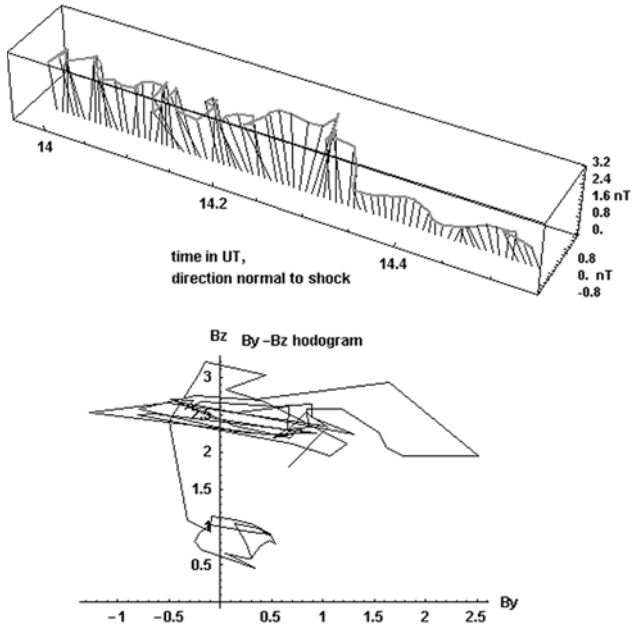

Figure 8. The upper plot shows the endpoints and directions of the magnetic field on DOY 012 between 1400 and 1433 UT. The magnetic field vectors are plotted as a function of time along the x-axis; this is the direction perpendicular to the shock front. The lower plot exhibits the hodogram in the B_y-B_z plane for the same period of time; both axes show the field strength in nT.

between 49° and 102°, and for the last one they were actuated between −79° and 101°. We attempted to correct the count rates by adding the missing values symmetrically to the distribution functions, but these did not change significantly either the SW velocities given above or the temperature data.

[38] We derived the shock normal direction from the quiet intervals before and after the perturbed regions a few hours apart (this is an uncertain method because the SW shown in Figure 2 does not support the assumption that it was quiet for hours). The shock on DOY 042 was parallel ($\theta_{Bn} \sim 2°$, $\mathbf{n}_{RTN} \sim \{-0.94, 0.3, 0.2\}$); the overall shape of the magnetic field supports this conclusion; this shock is a typical parallel turbulent shock transition. For DOY 045 we have ($\theta_{Bn} > 70°$, $\mathbf{n}_{RTN} \sim \{-0.3, 0.5, -0.8\}$). The shock on DOY 055 was oblique ($\theta_{Bn} \sim 50°$, $\mathbf{n}_{RTN} \sim \{-0.4, -0.8, 0.3\}$) outbound and quasi-parallel inbound. On DOY 057 we had ($\theta_{Bn} \sim 70°$, $\mathbf{n}_{RTN} \sim \{-0.1, -0.7, 0.7\}$). These yields as perpendicular Mach numbers (the ratio of the SW velocity perpendicular to the shock and v_A) ∼18 for DOY 042 and ∼9 for DOYs 045 and 055. From the known

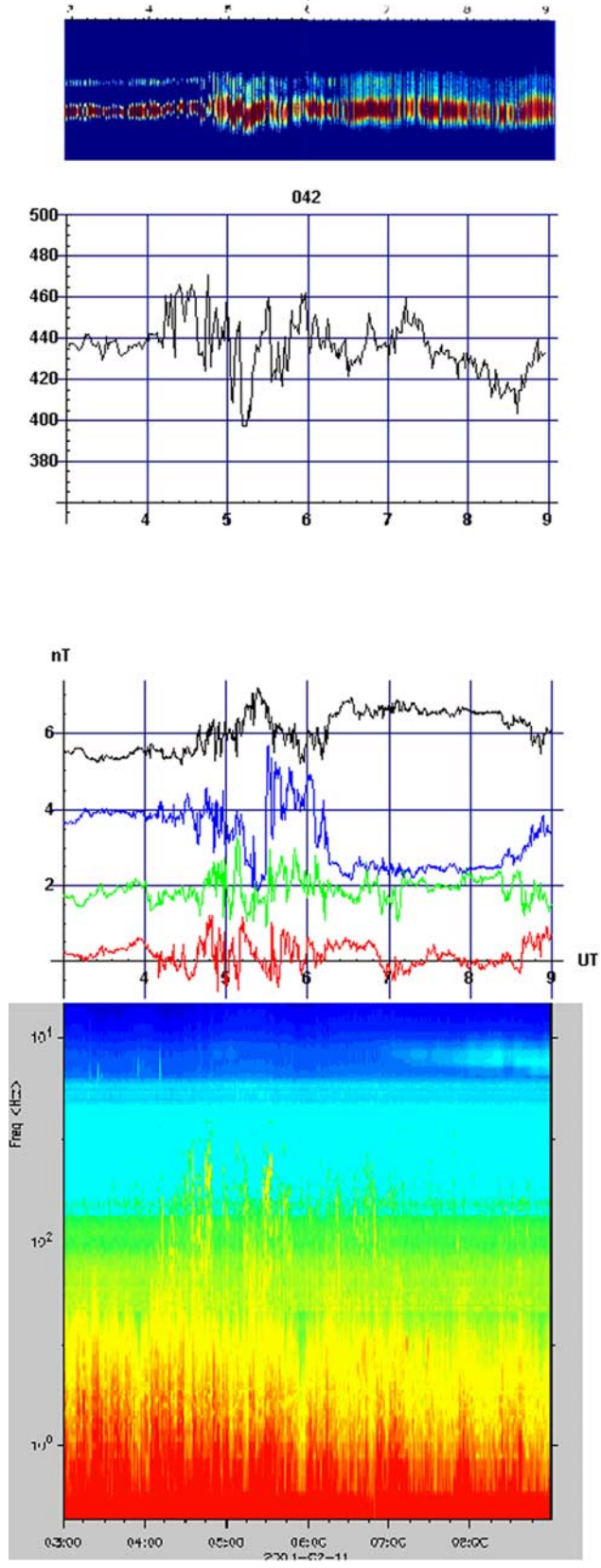

Figure 9. (opposite) A compilation of the plasma parameters for DOY 042, 0300–0900 UT. All horizontal axes show time in UT. The top panel shows the IBS energy spectra; the color code and scale are the same as shown in Figure 6. The top middle panels exhibits the bulk plasma velocity; the vertical scale is in km/s. The lower middle panels show the magnetic field data; the notations are the same as in Figure 4. The lower panel exhibits the wave data; the color scale is the same as in Figure 6.

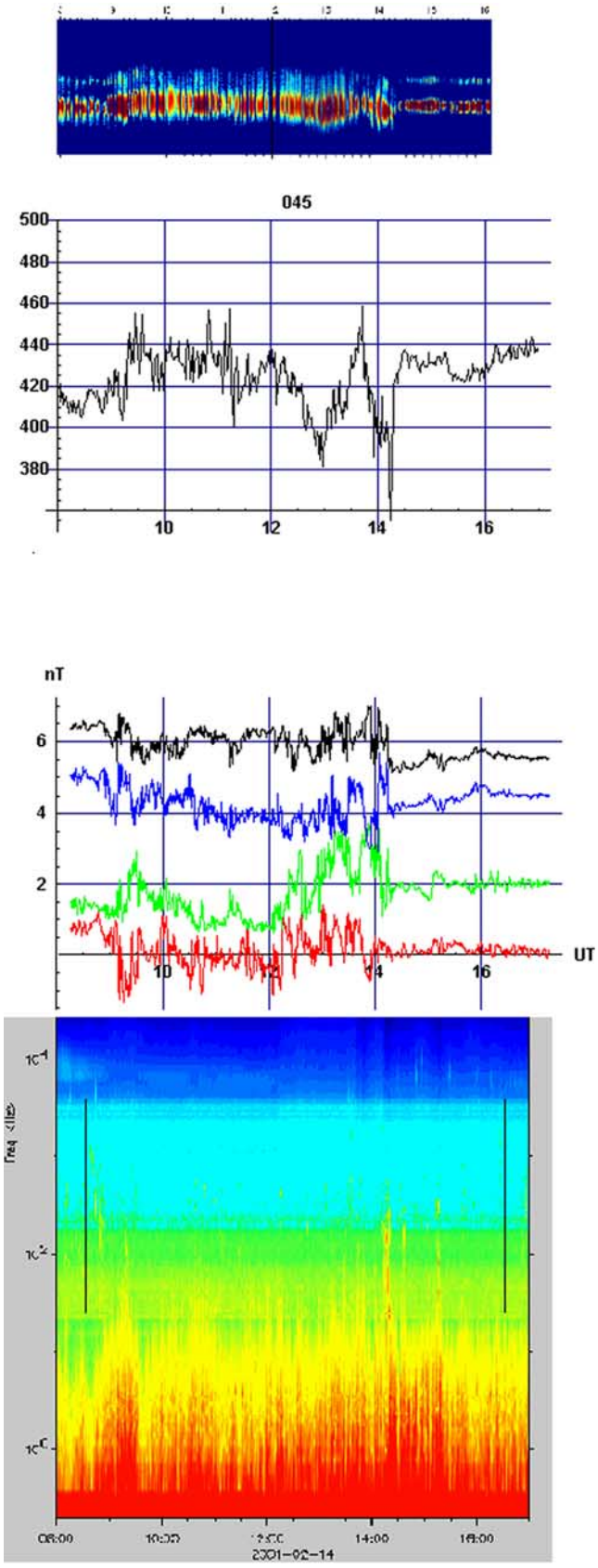

Figure 10. A compilation of the plasma parameters for DOY 045, 0800–1700 UT. The notations are the same as in Figure 9.

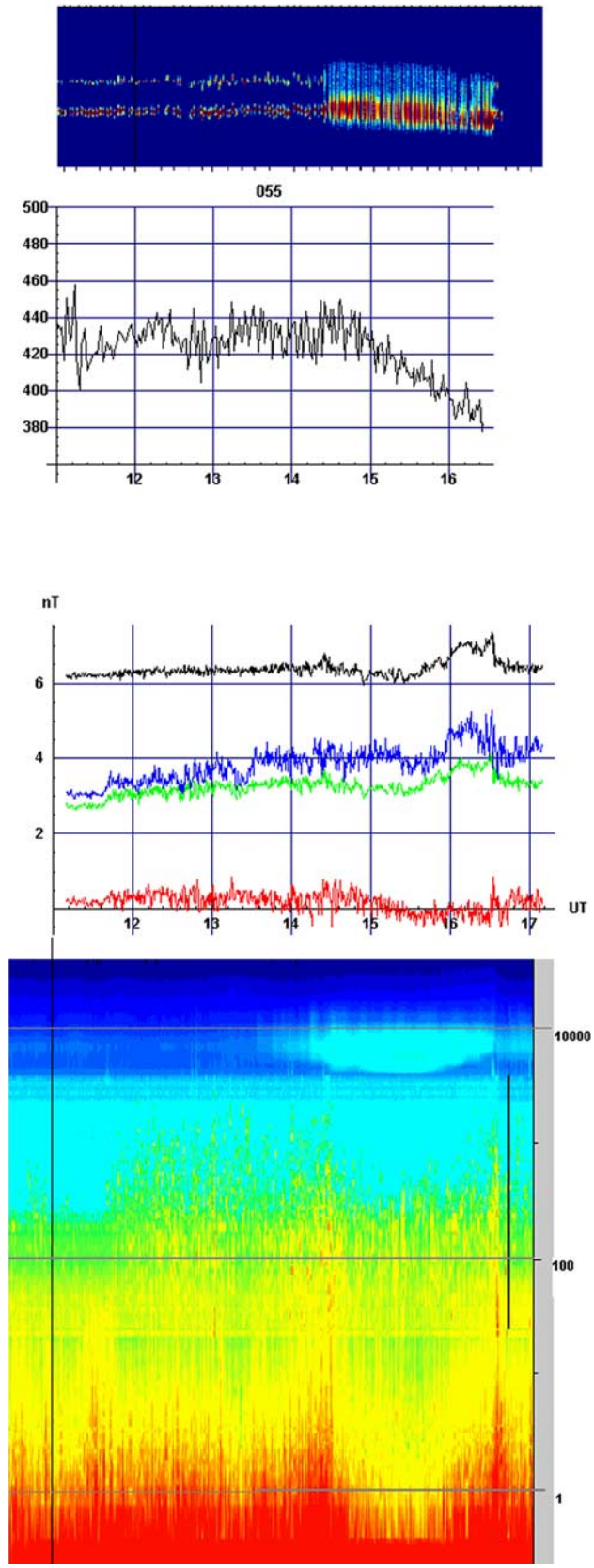

Figure 11. A compilation of the plasma parameters for DOY 055, 1000–1700 UT. The notations are the same as in Figure 9.

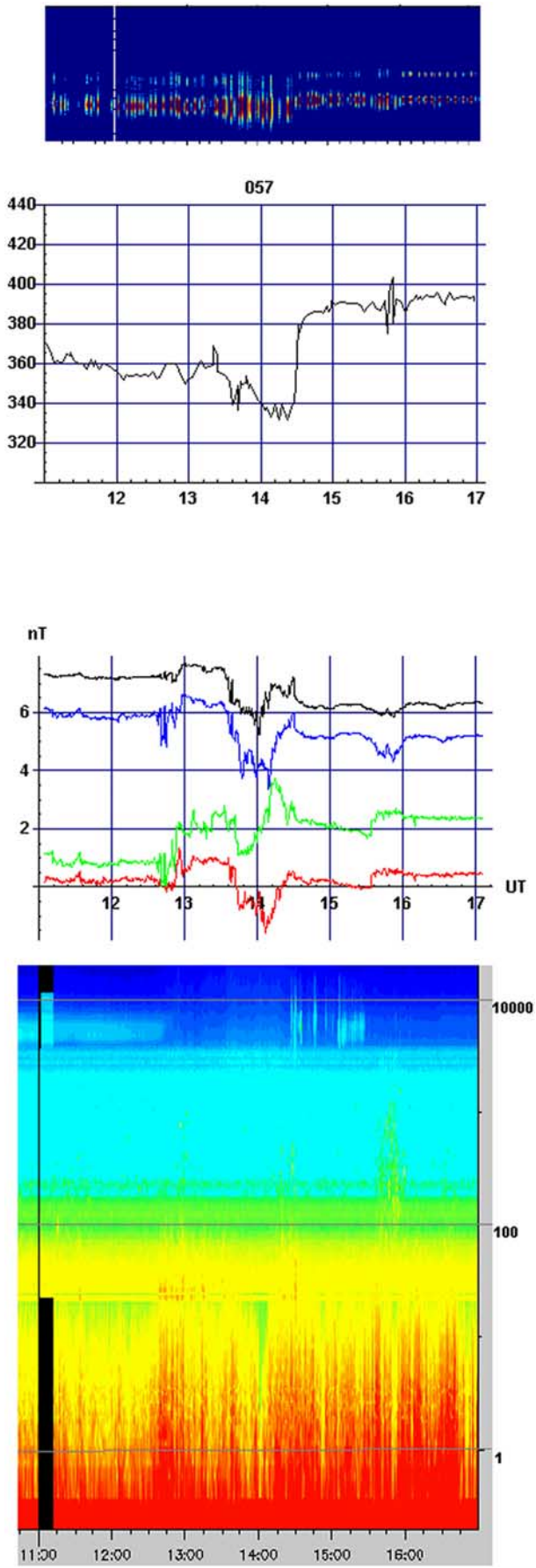

spacecraft velocity it is easy to calculate the angles between the spacecraft velocity vectors and the shock normals, these are 169°, 124°, 83°, and 70°, respectively.

[39] Many features of these shock transitions are beyond our understanding. On DOY 042 we expect strong wave activity in the foot region for a quasi-parallel shock, but the cause of the jump of the bulk plasma velocity is unclear; the same is true for its strong variation downstream. Both on DOY 042 and 045 the bulk plasma velocities downstream after the ramp make large excursions. The magnetic field values do not seem to support the hypothesis that the spacecraft crossed the shock front more than once during these intervals. The inbound shock crossing on DOY 055 is a quasi-parallel one; the outbound crossing is quasi-perpendicular. We have a gap in the SW data outbound, so it is difficult to comment on the slow bulk velocity decrease; it might be connected with the slow shock crossing as well. The DOY 057 crossing shows a bulk velocity jump quite typical for a perpendicular BS. However, the magnetic field variation is more complex: a substructure is evident between 1300 and 1330 UT, and in the downstream region the heating is so weak that the proton and alpha distributions are still resolved in E/q. The strength of the shock potential (neglecting the pressure gradient contribution) can be assessed from $1/2\ m(u^2_{up} - u^2_{down})$; this yields $\sim$100 eV, half of the shock potential on DOY 012; there is no significant difference between the four crossings we are considering here.

[40] Despite the perturbed conditions the ion heating is sudden and sharp in all four cases, accompanied by a density jump and an electrostatic spike in the wave data. Thermalization can be used as a signature of the shock location even in those cases when the field data are rather smeared; it is a good indicator of shock location.

[41] The wave activity is high during all crossings, but in the ion data there is no direct evidence for reflected ions; that is, no single count was detected outside the SW direction. If the reflected particles had been propagating along the upstream magnetic field, they would have fallen into the FOV of IBS; specularly reflected ions could have been seen only on DOY 045. In Figure 13 we plot the thermal velocities of the SW ions for DOYs 042 and 045. In both cases the temperature values show strong modulations (possibly associated with the instabilities in the foot), but we could not yet identify correlation with the field data. We return to this issue in the next section.

[42] Though the quiet upstream and downstream regions are separated by hours, the real microstructure and the actual width of these shocks are a question. Taking into account the low incidence angles and the $\sim$10 km/s spacecraft velocity, our preferred conclusion is that these shocks were exceptionally broad, but claims that only the crossing was slow cannot be excluded with certainty.

[43] The downstream ion distributions are generally perturbed: single- and bi-Maxwellian distributions can both be seen as illustrated in Figure 14. A difficulty here is that IBS does not resolve mass, so we could not be sure about the true composition of the second peak or the tail. We are of

Figure 12. (opposite) A compilation of the plasma parameters for DOY 057, 1000–1700 UT. The notations are the same as in Figure 9.

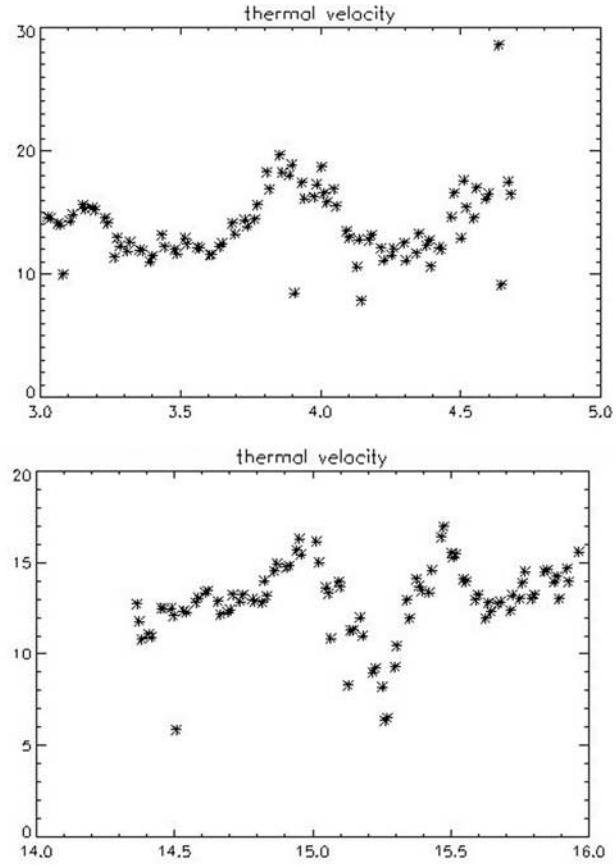

Figure 13. The solar wind thermal velocity for DOY 045 between 1420 and 1600 UT and for DOY 042 between 0300 and 0442 UT are shown. The horizontal axis exhibits time. The vertical axis is velocity in km/s.

the opinion, however, that this is the manifestation of the perturbed post-ramp distributions seen in numerical simulations [*Leroy et al.*, 1982] and many observations at the Earth's bow shock [e.g., *Montgomery et al.*, 1970].

[44] Strong magnetic turbulences are superimposed on the magnetic fields. To exhibit these, we rotate the magnetic field into a coordinate system in such a way that the shock normal is parallel to the x-component. As shown in Figure 15a, the magnetic field components are in phase between 1325 UT and 1355 UT. Similar large-scale structures were seen in the magnetic field structures on DOY 042, as shown in Figure 15b. *Andre et al.* [2002] has published an overview of the mirror mode fluctuations near Jupiter during the Cassini flyby. The magnetic structures seen on DOY 042, 1440–1450 UT, and on DOY 045, 1355–1400 UT, allow an interpretation that the fluctuations are mirror modes. However, the low time resolution of CAPS does not permit a correlation of the magnetic field and particle data for these short time intervals. The magnetic hodograms do not reveal any particular polarisation for the whole interval shown in the figures.

6. Discussion and Conclusions

[45] In this paper we have presented the first results of the measurements of the Jovian bow shock made by the charged particle analyser CAPS carried on board the Cassini spacecraft, together with supporting data from the magnetometer and the radio and plasma wave science instrument RPWS. We have provided an overview of the SW properties during the Jupiter flyby between 1 January and 30 March 2001, and we have discussed the structure of the transition layer of the Jovian bow shock, focusing on five crossings.

[46] Cassini encountered Jupiter during a high solar activity period. In the year 2000 and at the beginning of 2001 two magnetic sectors were present on the Sun up to high latitudes, divided by one single warped current sheet tilted slightly to the rotation axis of the Sun; the interplanetary magnetic field was significantly different from the low solar activity situation. The observed magnetic field structure indicates that Cassini several times crossed current sheet boundaries, and the SW velocity had a highly variable structure, as seen from the ACE data (cf., Figure 2). *Gurnett et al.* [2002a, 2002b] detected three interplanetary shocks (IPS) prior to the encounter between DOYs 320–360 in 2000; we reported an IPS on DOY 015, 2001, and other IPSs were also crossed during this 90-day long interval.

[47] The Jovian bow shock must differ significantly from that of the Earth. At the Earth the SW reaches the flank in a few minutes, and the time needed for the magnetohydrodynamical waves to travel between the obstacle and the bow shock is minutes. At Jupiter it requires days till the SW reaches the flank, and even at the nose the travel time can be hours. In addition, as pointed out by *Huddlestone et al.* [1998], the obstacle itself is a quickly changing magnetodisk. If we compare these time scales with the time scales of solar wind fluctuations, it is conceivable that the Jovian bow shock may seldom stay in a steady state, if it is reached at all. A further complication arises from the high Mach number because as *Quest* [1985] has pointed out, the normal energy dissipation mechanisms that stabilize Earth's bow shock might not be adequate. Therefore the high variability of the Jovian bow shock is not surprising. It is, however, a nontrivial question how this variability should be manifested. The drastically changing bow shock location, experienced by all previous missions and by Cassini as well, is such a signature, though it is also connected with the low sheath density, in proportion with the low solar wind density at Jupiter. Our intuition is driven here by a simple spring model; a softer but longer spring makes larger excursions but oscillates more slowly than a shorter and stronger one (the spring length is connected with the bow shock obstacle distance and the softness is connected with the sheath density). We suggest other possible signatures of an unsteady bow shock below, being aware that these have not yet been explored in detail theoretically.

[48] The Cassini spacecraft crossed the Jovian bow shock for the first time on 28 December 2000, at about 0419 UT. Owing to favourable coincidence of the solar wind dynamics and the spacecraft orbit, Cassini crossed the shock front about 40 more times in the ecliptic plane on the duskside. This side was not explored by the first four space missions targeting Jupiter, and because of the fast corotation of the Jovian magnetosphere, no trivial symmetry can be expected between the dawn and dusk sides. In this sense, even the phenomenological description of the bow shock crossings provides new, important insight. In this paper we have presented the detailed description of five BS crossings,

one around 1930 LT, other four between 2100 and 2200 LT. The Jovian bow shock is huge, extending over 700 R_J from the planet, and Cassini was the first spacecraft experiencing such distant bow shock crossings.

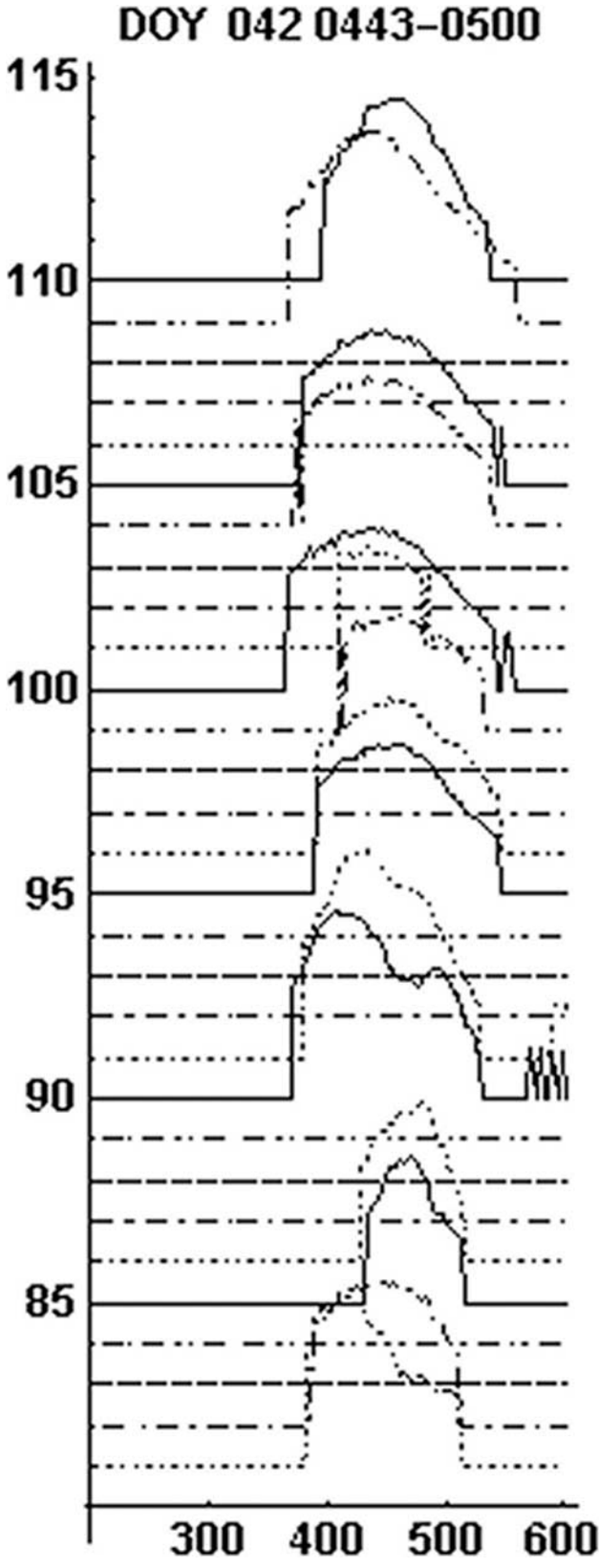

[49] An important conclusion is that even in those cases when the magnetic field and wave structures would not allow an easy determination of the shock location, the onset of proton thermalization is a good signature of it. The thermalization sets in at a very short characteristic time scale, accompanied by a jump in bulk plasma density. At the same location we have always observed a relatively strong electrostatic pulse in the proton plasma frequency range, possibly due to electrostatic ion waves [*Wu et al.*, 1984]. *Thomsen et al.* [1985] has found such fast proton thermalization at the ramp of the Earth bow shock for Mach numbers close to the critical value. They have argued that the bulk ion heating might be caused by modified two-stream instability driven by cross-field currents within the shock, and ion acoustic instability, driven by field-aligned beam. In those studies, however, the magnetic field was always a good indicator of the shock surface; therefore the question of whether thermalization is a good shock indicator even if the magnetic field is not was not raised. In our case all the shocks are supercritical, or the Mach numbers are even higher than the second critical Mach number. The picture we suggest is the following: in addition to the wave excitation modes described above, it is known that density gradient at the shock ramp can be the source of free energy for lower hybrid drift instabilities [cf., *Wu et al.*, 1984, equation (8)], and such lower hybrid waves can effectively heat ions. Though the details should be worked out, we suggest that the location of the density gradient manifests itself in lower hybrid wave excitation that subsequently heats ion. This is the reason why thermalization can be used to find the location of the ramp for high Mach number shocks.

[50] The next finding is that at the flanks, between 2100 and 2200 LT, the shock transition layer (defined as the region extending from quiet upstream to quiet downstream) is very much perturbed and broad. The energy loss of the bulk upstream particle population is about half of what was observed at 1930 LT. The weakening of the shock potential towards the flank in certain models is frequently associated with the decrease of the local Mach number derived from the component of the solar wind perpendicular to the shock front. *Lee and Wu* [2000, Figure 9] showed using hybrid simulations that the correlation between shock potential jump and shock Mach number is not linear; in their model the shock potential drops both for very high and very low Mach numbers. In our cases the Mach number was higher than at earlier local times, and the shock potential was much weaker.

[51] When we cross the bow shock the variation of the plasma parameters from the upstream regions to downstream more frequently defies expectations than otherwise. Whereas the Rankine-Hugoniot relations correctly described the bulk plasma properties in cases when the magnetic field indicated a clear discontinuity as well, in other cases the

Figure 14. (opposite) IBS velocity log counts spectra are shown. The horizontal axis is velocity in km/s units. The spectra, measured in each 32 s are shown in vertical arrangement; time flows upward. As the plasma flow is not always in the field of view of the actuator, there are ''zero-count'' spectra as well. The middle position of the actuator for these spectra, starting from below, are 93, 89, 64, 58, 80, 96, 80, 58, 63, 88, 92, 69, 56, 72, 94, 87, 62, 58, 80, 58, 80, 57, 62, 87, 93, 72, 57, 72, and 93 degrees.

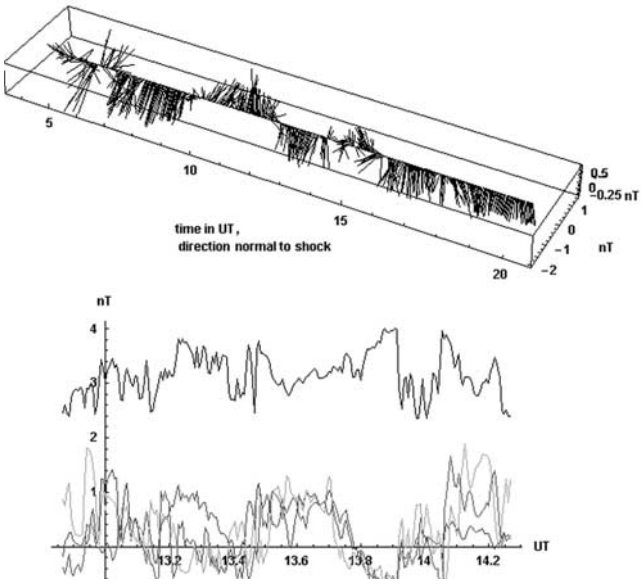

Figure 15. (a) The magnetic field perturbations downstream of the shock of DOY 045, when the x-component is along the shock normal. The horizontal axis is time in UT, and the vertical axis is magnetic field in nT. Shown are the x (red), z (blue), and −y (green) components of the magnetic field, the latter decreased by 1 nT. The black line is the total field, shifted by 2 nT upwards. (b) Long wavelength standing waves downstream of the shock on DOY 042. The horizontal axis is time in UT measured along the direction of the shock normal; the other axes are magnetic field components in nT.

bulk plasma velocity exceeds upstream velocity values within the shock transition layer and makes large excursions. We do not have any explanation of that or of the behavior of other fields and plasma parameters. These can certainly be associated with variations in the solar wind, but we believe that more complex explanation is needed. The bow shock seems to be very broad at the flank; further work is needed to find out the substructures seen in the transition layer.

[52] The high variability of the Jovian bow shock was confirmed by all previous missions. We are of the opinion that many of the observed features are indicative of the nonequilibrium state of the BS. In equilibrium, for quasi-perpendicular shocks, there is time for the wave steepening and for all the well-known shock structures to develop; probably the opposite is true for nonequilibrium. Therefore it is conceivable that the large variety of magnetic wave-like structures superimposed on the shock front might be connected with the lack of equilibrium. We have illustrated their presence in the paper. For the time being this is a conjecture only; we are not really aware of techniques that can treat such problems.

[53] Reflected protons were not detected upstream the bow shock above our current sensitivity limit. *Gosling and Robson* [1985] argued that particles are specularly reflected if their energy is lower than the shock potential. These are either returned to the shock front by the ambient magnetic field or they are streaming back upstream. A different population may propagate along the magnetic field lines [*Thomsen*, 1985]. Both directions were in our FOV on DOY 012, and the magnetic field direction was in the FOV for all cases. Therefore it is somewhat surprising that we did not detect them because about a quarter of the protons should have been reflected. Our explanation is that the reflected protons are expanding quickly in the phase space, and even though CAPS looked into the right directions, the particle densities were below the sensitivity threshold. Wave data collected in the foot region of the bow shock indicate the presence of a reflected particle distribution. In the foot region the SW becomes perturbed, and its temperature is modulated. In the simulation of *Quest* [1985], fluctuations in reflected particle distributions indicate shock instability when the Mach number is high. The observed SW temperature fluctuations (with $M_A \sim 18$ in one case) might be connected with this fact. We do not discuss further foot phenomena here, but this will be the topic of separate publications.

[54] In summary, in this paper we have presented the phenomenology of the Jovian bow shock as observed by the CAPS instrument onboard the Cassini spacecraft. Cassini explored the duskside of the bow shock in the ecliptic plane, which was not visited by previous missions. No previous mission observed such an extended shock, still present more than 700 R_J away from Jupiter. The shock transition layer at the flank was broad and very much perturbed, but the onset of the ion thermalization, accompanied by a fairly strong electrostatic wave pulse and a jump in bulk plasma density, was always fast. The bulk plasma behaviour in the broad transition layer is not understood yet. In the foot region the reflected ions were below CAPS sensitivity limit; their presence however is suggested by the field data and by the observed changes in the solar wind. We have conjectured that most of the observations indicate an unsteady bow shock, but the physical interpretation of the observation will be the focus of future works.

[55] **Acknowledgments.** The work of K. S. was supported by the Hungarian OTKA grant T-32634. The research at The University of Iowa was supported by NASA through contract 961152 through the Jet Propulsion Laboratory. Work at MSSL-UCL was supported by PPARC.

[56] Lou-Chuang Lee thanks B. H. Wu and another reviewer for their assistance in evaluating this paper.

References

Andre, N., G. Erdos, and M. K. Dougherty, Overview of mirror mode fluctuations in the jovian dusk magnetosheath: Cassini magnetometer observations, *Geophys. Res. Lett.*, *29*(20), 1980, doi:10.1029/2002GL015187, 2002.

Balogh, A., M. K. Dougherty, R. J. Forsyth, D. J. Southwood, E. J. Smith, B. T. Tsurutani, N. Murphy, and M. E. Burton, Magnetic field observations during the Ulysses flyby of Jupiter, *Science*, *257*, 1515–1518, 1992.

Bame, S. J., et al., Jupiter's magnetosphere: Plasma description from the Ulysses flyby, *Science*, *257*, 1539–1543, 1992.

Cravens, T. E., *Physics of Solar System Plasmas*, Cambridge Univ. Press, New York, 1997.

Dougherty, M. K., et al., The Cassini magnetic field investigation, *Space Sci. Rev.*, in press, 2002.

Gosling, J. T., and A. E. Robson, Ion reflection, gyration, and dissipation at supercritical shocks, in *Collisionless Shocks in the Heliosphere: Review of Current Research*, *Geophys. Monogr. Ser.*, vol. 35, edited by B. T. Tsurutani and R. G. Stone, pp. 141–152, AGU, Washington, D. C., 1985.

Gurnett, D. A., et al., Control of Jupiter's radio emission and aurorae by the solar wind, *Nature*, *415*, 985, 2002a.

Gurnett, D. A., et al., The Cassini radio and plasma wave investigation, *Space Sci. Rev.*, in press, 2002b.

Hill, W. H., Magnetic moments at Jupiter, *Nature*, *415*, 965, 2002.
Huddlestone, D. E., C. T. Russell, M. G. Kivelson, K. K. Khurana, and L. Bennett, Location and shape of the Jovian magnetopause and bow-shock, *J. Geophys. Res.*, *103*, 20,075–20,082, 1998.
Kivelson, M. G., et al., Galileo at Jupiter: Changing states of the magnetosphere and first looks at Io and Ganymede, *Adv. Space Res.*, *20*, 193–204, 1997.
Kurth, W. S., et al., An overview of observations by the Cassini radio and plasma wave investigation at Earth, *J. Geophys. Res.*, *106*, 30,239, 2001.
Lee, L. C., and B. H. Wu, Heating and acceleration of protons and minor ions by fast shocks in the solar corona, *Astrophys. J.*, *535*, 1014–1026, 2000.
Leroy, M. M., et al., The structure of perpendicular bow shock, *J. Geophys. Res.*, *87*, 5081, 1982.
Lever, E. L., et al., Shock surfing versus shock drift acceleration, *Geophys. Res. Lett.*, *28*, 1367, 2001.
Linder, D. R., et al., The Cassini CAPS electron spectrometer, in *Measurement Techniques in Space Plasmas: Particles*, *Geophys. Monogr. Ser.*, vol. 102, edited by R. Pfaff, J. Borovsky, and D. Young, pp. 257–262, AGU, Washington, D. C., 1998.
Montgomery, M. D., J. R. Asbridge, and S. J. Bame, Vela 4 plasma observations near the earth's bow shock, *J. Geophys. Res.*, *75*, 1217, 1970.
Moses, S. L., F. V. Coroniti, C. F. Kennel, and F. L. Scarf, Estimation and comparison of quasilinear electron heating in the shock foot at Jupiter and Earth, *Geophys. Res. Lett.*, *12*, 609–612, 1985.
Moses, S. L., F. V. Coroniti, C. F. Kennel, W. S. Kurth, and D. A. Gurnett, Comparison of plasma wave measurements in the bow shocks at Earth, Jupiter, Saturn, Uranus and Neptune, *Geophys. Res. Lett.*, *17*, 1653, 1990.
Quest, K. B., Simulation of high Mach number collisionless perpendicular shocks in astrophysical plasmas, *Phys. Rev. Lett.*, *54*, 1872–1874, 1985.
Scarf, F. L., D. A. Gurnett, and W. S. Kurth, Measurements of plasma wave spectra in Jupiter's magnetosphere, *J. Geophys. Res.*, *86*, 8181–8198, 1981.
Scarf, F. L., S. L. Moses, C. F. Kennel, E. W. Greenstadt, and F. V. Coroniti, Plasma waves near collisionless shocks, in *Proceedings of the International Conference on Collisionless Shocks in Balatonfured, Hungary*, edited by K. Szego, pp. 19–41, Cent. Res. Inst. for Phys., Budapest, Hungary, 1987.
Scudder, J. D., E. C. Sittler, and H. S. Bridge, A survey of the plasma electron environment of Jupiter: A view from Voyager, *J. Geophys. Res.*, *86*, 8157–8179, 1981.
Smith, E. J., et al., Ulysses in the south polar cap at solar maximum: Heliospheric magnetic field, *Geophys. Res. Lett.*, *28*, 4159, 2001.
Stone, R. G., et al., Ulysses radio and plasma wave observations in the Jupiter environment, *Science*, *257*, 1524–1531, 1992.
Thomsen, M. F., Upstream suprathermal ions, in *Collisionless Shocks in the Heliosphere: Review of Current Research*, *Geophys. Monogr. Ser.*, vol. 35, edited by B. T. Tsurutani and R. G. Stone, pp. 253–270, AGU, Washington, D. C., 1985.
Thomsen, M. F., J. T. Gosling, S. J. Bame, and M. M. Mellott, Ion and electron heating near the critical Mach number, *J. Geophys. Res.*, *90*, 137–148, 1985.
Wu, C. S., et al., Microinstabilities associated with a high Mach number, perpendicular bow shock, *Space Sci. Rev.*, *37*, 63, 1984.
Young, D. T., et al., Cassini plasma spectrometer investigation, in *Measurement Techniques in Space Plasmas*, Geophys. Monogr. Ser., vol. 102, edited by R. E. Pfaff, J. E. Borovsky, and D. T. Young, pp. 237, AGU, Washington, D. C., 1998.
Young, D. T., et al., Cassini plasma spectrometer investigation, *Space Sci. Rev.*, in press, 2002.
Vilppola, J. H., P. J. Taskanen, B. L. Barraclough, and D. J. McComas, Comparison between simulations and calibrations of a high resolution electrostatic analyzer, *Rev. Sci. Instr.*, *72*, 3662–3669, 2001.

B. Barraclough and M. F. Thomsen, Los Alamos National Laboratory, Space and Atmospheric Science Group, Los Alamos, NM 87545, USA. (bbarraclough@lanl.gov; mthomsen@lanl.gov)

J.-J. Berthelier, Centre d'Étude des Environnements Terrestre et Planetaires, Observatoire de Saint-Maur, 4 Avenue de Neptune, 94107 St. Maur-des-Fosses Cedex, France. (jean-jacques.berthelier@cetp.ipsl.fr)

F. J. Crary, University of Michigan, 2455 Hayward Street, Ann Arbor, MI 48109, USA. (fcrary@umich.edu)

A. J. Coates, University College London, Mullard Space Science Laboratory, Holmbury St. Mary, Dorking, Surrey RH5 6NT, UK. (ajc@mssl.ucl.ac.uk)

M. K. Dougherty, Blackett Laboratory, Imperial College, Prince Consort Road London, SW7 2 BW, UK. (m.dougherty@ic.ac.uk)

G. Erdos and K. Szego, KFKI Research Institute for Particle and Nuclear Physics, Konkoly Thege str. 29-33, Bldg. III, H-1121 Budapest, Hungary. (erdos@rmki.kfki.hu; szego@rmki.kfki.hu)

D. A. Gurnett and W. S. Kurth, Department of Physics and Astronomy, The University of Iowa, 203 Van Allen Hall, Iowa City, IA 52242-1479, USA. (donald-gurnett@uiowa.edu; william-kurth@uiowa.edu)

D. J. McComas and D. T. Young, Division of Space Sciences and Engineering, Southwest Research Institute, 6220 Culebra Road, P. O. Drawer 28510, San Antonio, TX 78228-0510, USA. (dmccomas@swri.edu; dyoung@swri.ed1u)